ACADEMIA ROMÂNĂ
Revue Roumaine de Chimie
http://web.icf.ro/rrch/

Rev. Roum. Chim.,
2018, *63*(5-6), 407-417

Dedicated to Dr. Maria Zaharescu
on the occasion of her 80th anniversary

PRISTINE AND Au-MODIFIED ZnO *vs.* TiO_2 NANO-POWDERS PREPARED BY SOL-GEL: SYNTHESIS, STRUCTURAL PROPERTIES AND PHOTOCATALYTIC DEGRADATION OF RHODAMINE B**

Susana MIHAIU, Oana Cătălina MOCIOIU, Luminita PREDOANA, Irina ATKINSON,* Silviu PREDA, Cristina VLADUT, Ecaterina TENEA, Mihai STOICA, Jeanina CUSU-PANDELE, Crina ANASTASESCU, Jose M. CALDERON-MORENO, Mihai ANASTASESCU,* Mariuca GARTNER and Ioan BALINT

"Ilie Murgulescu" Institute of Physical Chemistry of the Roumanian Academy, 202 Splaiul Independenței, 060021 Bucharest, Roumania

Received August 7, 2017

ZnO nano-powders have been prepared by sol-gel method, alcoholic route, starting from zinc acetate dihydrate as Zn source. The obtained white powders where thermally treated (TT) at 400 and 500 °C for 1h. The modification of ZnO powder with Au was performed by impregnating it with 0.2 mM aqueous solution of chloroauric acid followed by TT at 500 °C in air stream for 1 hour. The characterization of the ZnO powders was made by TG/ATD analysis, X-ray diffraction, FT-IR spectroscopy and Scanning Electron Microscopy. X-ray diffraction analysis of the nano-powders revealed a hexagonal wurtzite ZnO phase and the presence of Au in the Au-modified ZnO powder TT at 500 °C. FT-IR spectra identified the Zn-O characteristic bands and the change of shape and intensity of bands with crystallization. The temperature of 500°C and addition of Au have positive influence on crystallization. TiO_2 was used as reference photocatalyst for photoreactivity evaluation of the ZnO-based materials, and it was synthesized also by sol-gel method starting from titanium isopropylate. According to the thermal analysis investigations, the TiO_2 powder was thermally treated at 400 °C for 1h, leading to the crystallization into the anatase phase, as proved by XRD. SEM revealed the morphology of the TiO_2 powder and FT-IR the characteristic vibrational bands of the obtained material. Both materials, ZnO and TiO_2, have similar fine grains but with different aggregation tendency. The photocatalytic evaluation of the obtained materials was been carried out for Rhodamine B (RhB) degradation under simulated solar irradiation, by following the transformation degree of the dye in time. It was found that Au enhances the photocatalytic degradation of the RhB, the pristine ZnO having comparable activity with TiO_2.

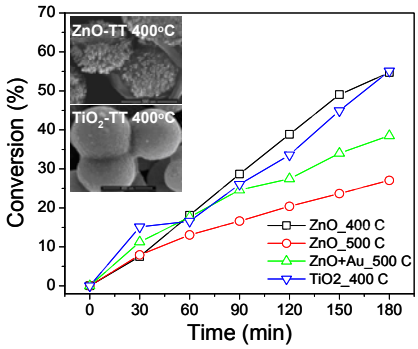

INTRODUCTION

Recently, the environmental degradation has raised significant awareness because of a great variety of residual compounds which can reach harmful levels in water, soil and air, affecting the quality of human and other living organism life. The degradation of organic pollutants, including dyes, from the aqueous medium using the solar irradiation which is a green energy source and semiconductor photocatalysts is already a widely studied issue but still open for further investigations, like the transformation of the organic pollutants into nontoxic products (desirable mineralization).

Zinc Oxide (ZnO) is a multifunctional material with interesting physical and chemical properties,

* Corresponding authors: manastasescu@icf.ro, irinaatkinson@yahoo.com

** This work is dedicated to Acad. Maria Zaharescu on the occasion of her80th anniversary for significant contributions towards the development of sol-gel materials chemistry

such as: high chemical stability, low toxicity and high electrochemical coupling.[1,2] ZnO is a large band-gap semiconductor (3.37 eV), large exciton binding energy (60 meV) and high thermal and mechanical stability at room temperature, making it attractive for many applications including electronics, optoelectronics and even laser technologies.[3,4] ZnO can be used as photocatalyst for degradation of organic pollution, hydrogen production, reduction of CO_2, sensor, converter, power generator, etc.[5,6] However, the application as a photocatalyst of ZnO is restricted to UV light due to its wide band gap (3.37 eV), and the fast recombination rate of photogenerated electron–hole pairs.[7] In order to overcome this limitation, loading of noble metallic nanoparticles on semiconductor seems to be a potential strategy for suppressing electron–hole pair recombination rate, extending the light absorption from UV to the visible region for developing light captors[8] and enhancing photocatalytic efficiency.[9] Several research groups have reported a higher photocatalytic activity when noble metallic nanoparticles (such as Au, Ag, and Pt) were deposited on ZnO nanostructures [10,11] mainly due to the surface plasmon resonance (SPR) phenomenon.

It is also well known that ZnO can display different (numerous) nanostructures and morphologies emphasizing specific physical, chemical and textural proprieties such a narrower energy band gap or higher surface area than non-nanostructured materials [6,9]. According to this, the photocatalytic activity of ZnO based materials strongly depends on the size and shape of the synthesized ZnO nanostructures but also of the modifier characteristics (doping material).

There are many methods of preparing ZnO, such as chemical deposition of the metal-organic vapor phase, atomic layer deposition, sol-gel method, spray pyrolysis, sputtering and laser ablation.[12] Among them, the sol-gel method offers several advantages, namely easier control of the materials obtained, the possibility of deposition on complex-shaped substrates, easier control of the dopant concentration, structural homogeneity, the relatively low temperature of the heat treatment, as well as the low cost of chemicals and equipment used.[13,14] For this reasons, is an appropriate method for versatile and low cost synthesis of ZnO powders and films. The same method was also intensively exploited to obtain multifunctional TiO_2-based materials, successfully applied in various fields such as photocatalysis, gas sensors, optical coatings, dye sensitized solar cells, antimicrobial agents, pigments, so on [15, 16].

In this work we report the comparative sol gel synthesis and characterization of pristine and Au modified ZnO powders, but also of sol gel TiO_2 powder as reference photocatalyst. The photocatalytic activity of the synthesized materials for the degradation of Rhodamine B was performed under simulated solar light. It was found that Au modified ZnO thermally treated at 500 ^oC sample is more active for Rhodamine B photodegradation than the unmodified one. On the other hand, the photoreactivity of pristine TiO_2 and ZnO samples, calcined at 400 ^oC, is slightly higher than for ZnO powders calcined at 500 ^oC.

EXPERIMENTAL

1. ZnO preparation

Pristine ZnO: The precursor solution for obtaining ZnO powders with 0.5 M zinc ions concentration was prepared starting from zinc acetate dihydrate (p.a. Merck) as a source of Zn^{2+}, triethanolamine (p.a. Baker Analyzed) as a chelating agent and catalyst, and Absolute ethanol (p.a. Merck) as solvent, with a molar ratio of zinc acetate triethanolamine / absolute ethanol of 5 / 1/154. The solutions were obtained by magnetic homogenization for 2 hours at 50 °C. By storing the solution at room temperature in the atmosphere, after complete evaporation of the solvent, a white amorphous powder was obtained. The powder obtained was thermally treated at 400 °C and 500 °C respectively, for one hour.

Au-modified ZnO: The modification of the ZnO powder with Au was performed by impregnating with 0.2 mM $HAuCl_4$ $3H_2O$ solution (in order to obtain a 0.14 wt % Au loading) under magnetic stirring for 2h, followed by heat treatment at 500 ^{o}C for 3 h in air stream.

The TiO_2 powder, used as reference photocatalyst for photoreactivity evaluation of ZnO-based materials, was also obtained by sol-gel method, using titanium isopropylate - $Ti(OC_2H_5)_4$ as precursor for Ti, alcohol as solvent, water as hydrolysis reagent and nitric acid (HNO_3) as catalyst. According to the thermal analysis investigations, the TiO_2 powder was thermally treated at 400 ^oC for 1h, leading to the crystallization into the anatase phase. The morphology of the TiO_2 materials was evidenced by SEM measurements while its structural characteristics were followed by FT-IR.

2. Characterization methods

Thermal behavior of the as-prepared powders was followed by a Mettler Toledo TGA / SDTA 851^e apparatus with a heating rate of 5 °C / min.

Formation of ZnO and TiO_2 specific bonds was evidenced by FTIR Spectroscopy using a Nicolet 6700 apparatus in the range 400-4000 cm^{-1}. All spectra were recorded on KBr pellets with 1 mg powder ZnO and 200 mg KBr. The sensibility of apparatus was 4 cm^{-1}.

The crystalline structure of pristine and Au modified ZnO powders was investigated by X-ray diffraction using a Ultima IV apparatus, Rigaku Co. Ltd., Japan with CuK radiation and using the experimental data analysis software produced by Rigaku (PDXL).

The morphology of the ZnO and TiO_2 powders was revealed by scanning electron microscopy (SEM) using a field emission FEI 3D microscope, operating at 20 kV.

The optical properties of the ZnO-based materials have been assessed by UV-VIS spectroscopy with a Perkin Elmer Lambda 35 spectrophotometer equipped with integrating sphere, in the 200-1100 nm wavelengths domain. The band gap energy was calculated from the Kubelka-Munk function.

The photocatalytic activity of the materials was tested using a quartz reactor filled with 120 mL of Rhodamine B solution having an initial concentration of 10 mg / L and 0.1 g of a slurry catalyst (ZnO or TiO_2 powder). The suspended solution catalyst was irradiated with a 4.5 x 4.5 cm^2 luminous flux generated by a solar light simulator (PECEL-L 01, Japan) equipped with a 150 W Xe lamp, emitting in the range of 350-1100 nm. During the photocatalytic tests, the reactor is purged with Ar (carrier gas). The evolution of the concentration of Rhodamine B over time was achieved by analyzing samples taken every 30 minutes using a UV-VIS-Analtik Jena Specord 200 Spectrophotometer.

RESULTS AND DISSCUSION

1. Characterization

1.1. Thermal analysis

The thermal and thermo-gravimetric curves for the powders are presented in Fig. 1. The thermal analysis of the as-prepared ZnO powder (without thermal treatment) – Fig. 1a – was performed in a temperature range from room temperature up to 600 °C in order to establish the proper thermal treatment of the obtained materials, leading to a crystalline reproducible structure. The TG curve indicates a step wise decomposition with a weight loss of app. 65% up to 500 °C. In the DTA curves the endothermic effects at 74 and 146°C are assigned to the desorption of ethanol and water. In the range of temperature 20-105 °C the elimination of water and ethanol takes place with a corresponding weight loss of around 3%, accompanied by a small endothermal effect with the maximum at 74 °C. Between 105 and 330 °C it can be observed that the decomposition of reagents takes place in an endothermic reaction (146, 233 and 305 °C) with a corresponding mass loss of around 48%. Also, between 350 and 500°C the mass loss is 14% accompanied by an exothermal effect at 437 °C assigned to the residual organics are burned out.

The thermal analysis of the ZnO powder thermally treated at 400 °C (Fig. 1b) was performed in a temperature range from room temperature up to 600 °C. The TG curve indicates a weight loss of approx. 3.5% up to 500 °C while the DTA curve an exothermic effect at 422 °C. Weight loss correlated with the presence of exothermic effect is due to the oxidation of the rest of the organics from the sample.

According to the thermal and thermo-gravimetric analysis, the ZnO powders were calcined at 400 and 500 °C, and their catalytic performances have been evaluated and compared with undoped TiO_2 also prepared by sol-gel and calcined at 400 °C. One batch of ZnO powder has been additionally modified with 0.14% Au and thermally treated at 500 °C, in an attempt to improve the photocatalytic behavior of the material towards RhB decomposition.

1.2. FT-IR spectroscopy

Pristine and Au modified ZnO powders were characterized from structural point of view by FTIR spectroscopy. In Fig. 2 the FTIR spectra are presented. The spectrum of ZnO sample thermally treated at 400°C indicates the presence of a wide band with maximum at 436 cm^{-1} which is attributed to Zn-O-Zn bond in wurtzite structure of ZnO, as the authors shown in previous paper [17, 18]. Also, the presence of water adsorbed on the surface can be associated [19] with the band appeared around 3400 cm^{-1} which is missing in the case of the samples treated at 500 °C.

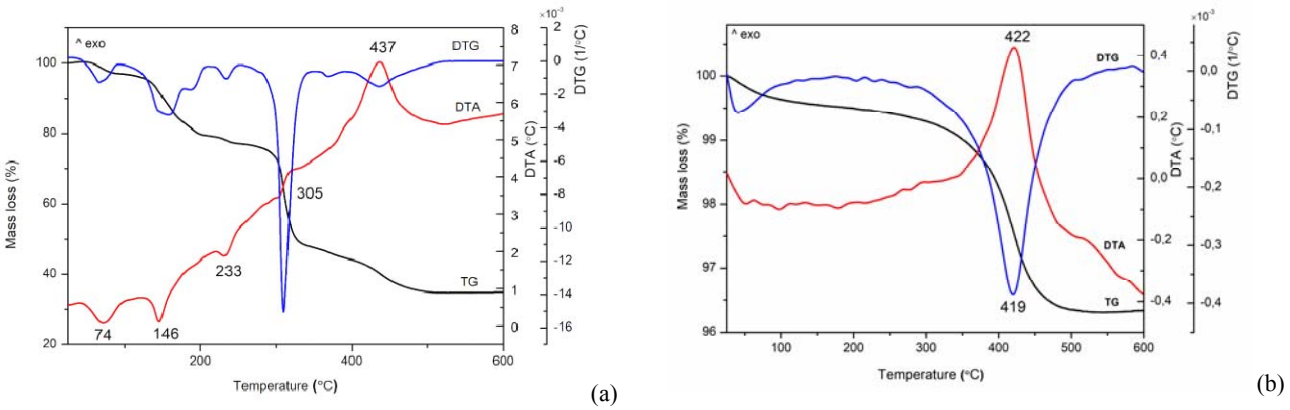

Fig. 1 – ATD, DTG and TG curves for the ZnO powders:
as-prepared powder (a) and thermally treated at 400 °C (b).

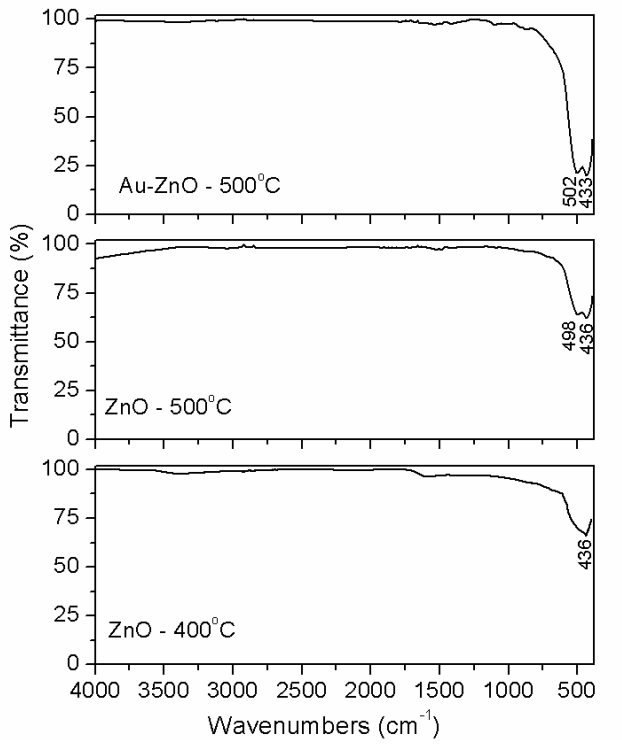

Fig. 2 – FTIR Spectra of ZnO and ZnO-Au powders.

In addition, in the case of ZnO sample thermally treated at 500°C, a second band at 498 cm^{-1} characteristic to Zn-O appeared. Further, it can be observed that the intensity of main bands is increasing for Au modified ZnO sample thermally treated at 500°C, which emphasizes an increasing of ZnO crystallization with the temperature, in agreement with Tian *et al.*[20] which identified the following sequence of crystallization with temperature: ZnO (400 ^oC) < ZnO (600 ^oC) < ZnO (800 ^oC) < ZnO (900 ^oC). The bands are shifted from 498 cm^{-1} and 436 cm^{-1} in ZnO powder to 502 cm^{-1} and 433 cm^{-1} in Au-modified ZnO powder, which can be correlated to a possible interaction between ZnO and Au.

Briefly, the FTIR spectra reveal an increasing of crystallization with calcinations temperature (500 °C) and Au addition (in good agreement with XRD measurements presented below), but also the disappearance of the adsorbed water for the sample treated at 500 ^oC.

1.3. X-ray diffraction

The XRD patterns of the obtained samples are presented in Fig. 3.

The pristine ZnO samples TT at 400^o and 500^o C reveal the diffraction lines identified as (100), (002), (101), (102), (110), (103),(112) and (201) planes of reflections of hexagonal wurtzite structure of ZnO in agreement with data from JCPDS card no. 36-1451. The XRD pattern of Au modified ZnO powder thermally treated at 500^{o}C shows additional diffraction lines corresponding to Au at 2θ of 38.12°, 44.36° and 64.62° (JCPDS card no. 71-4614). An increase of reflection intensity in the Au modified ZnO sample was observed as compared to the samples without Au addition. Lattice constants were calculated using PDXL software and the results are listed in Table 1 together with estimated standard deviation (in the brackets). Furthermore the average crystallite size (D) was estimated using Williamson-Hall method (Table 1). No significant changes of lattice constants against the values in the standard data (JCPDS 36-1451) were observed for the studied samples.

1.4. ZnO morphology (SEM)

The morphology of the undoped ZnO powders – Fig. 4 – was investigated by scanning electron microscopy (SEM) measurements.

As can be seen from Fig. 4, the morphology of ZnO powders is predominantly globular (Fig. 4a), and from the high resolution image (Fig. 4b) it can be seen that each spherical formation (average diameter 500 nm) has a fine nanoparticle structure in agreement with XRD results.

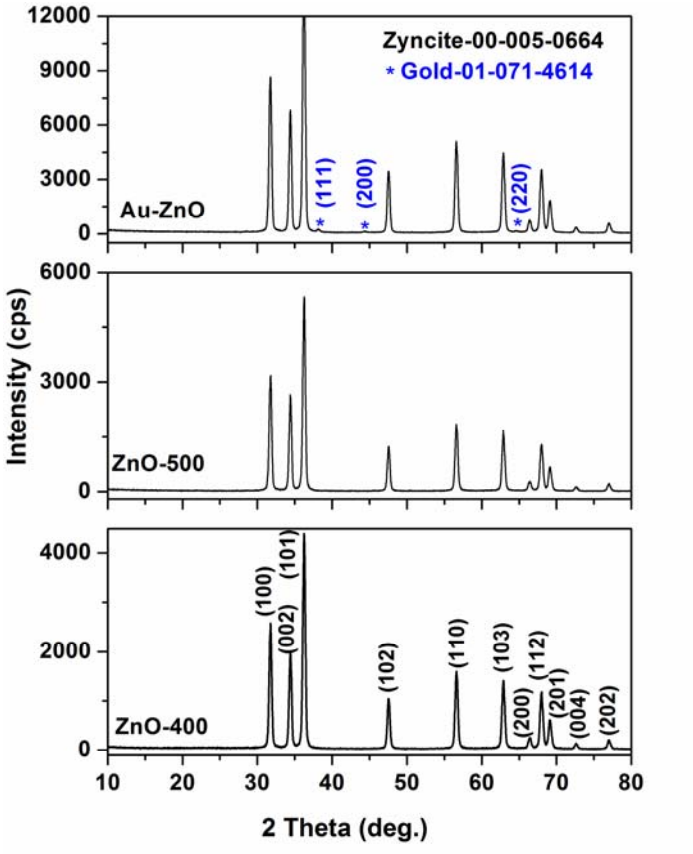

Fig. 3 – XRD patterns of the obtained samples.

Table 1

Lattice constants and crystallite size of the obtained samples

Sample	Phase	a=b (Å)	c (Å)	D (Å)
ZnO-400 ^{o}C	ZnO	3.250(3)	5.206(5)	217(1)
ZnO-500 ^{o}C	ZnO	3.251(1)	5.207(3)	222(3)
Au-ZnO-500 ^{o}C	ZnO	3.252(3)	5.209(7)	216(4)
ZnO JCPDS card no. 36-1451		3.249	5.206	-

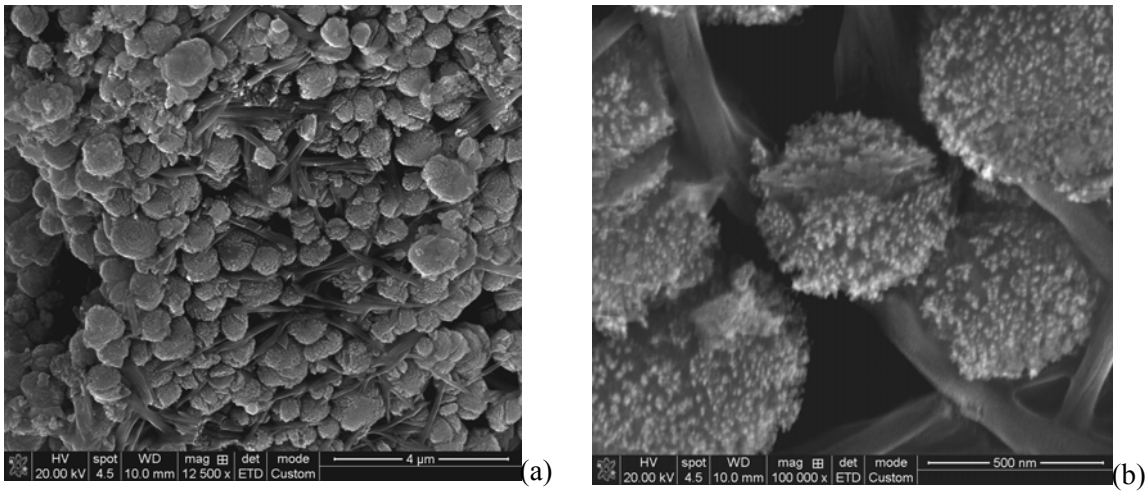

Fig. 4 – Morphology of ZnO powders treated at 400 ^{o}C at two different magnification scales: 12.5 k (a) and 100 k (b).

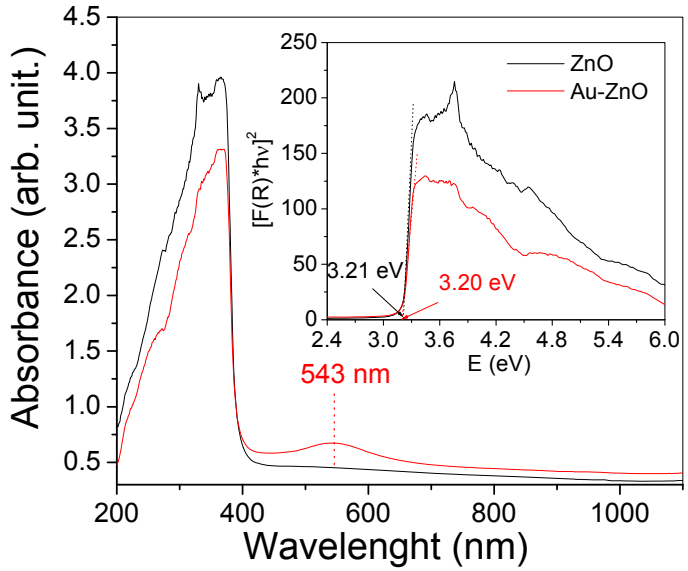

Fig. 5 – UV-VIS absorption spectra of the pristine and Au-modified ZnO powders thermally treated at 500 °C. Inset: The Kubelka-Munk plot of the same samples.

1.5. Optical properties of ZnO-based materials (UV-VIS)

Fig. 5 shows the optical absorption spectra of the pristine and Au-modified powders as obtained from UV-VIS spectroscopy.

The inset represents the Kubelka-Munk plot of the same materials used to evaluate the optical band-gap of the obtained powders. As could be observed, from Fig. 6, the absorption edge (the band-gap) is not influenced by the presence of Au in the ZnO matrix. On the other hand, Au exhibits its finger print in the Au-ZnO powder by the presence of the plasmonic peak, located in the visible range, at ~ 543 nm. The optical band-gap of both materials, as evaluated from the Kubelka-Munk plot, has a value of ~ 3.2 eV.

1.6. TiO_2 characterization (TG/DTG/DTA, XRD, SEM and FTIR)

The TiO_2 powder, used as a reference material for the photocatalytic performances of the ZnO-based materials, was characterized by TG/DTG/DTA, XRD and SEM (Fig. 6). The thermal behavior of the resulted materials was investigated by TG/DTG/DTA method (Fig. 6a). It could be noticed on the TG curves a step wise decomposition in the 20-380 °C temperature range, with a noticeable total weight loss around 22%. In the range of temperature 20-105 °C the elimination of water takes place with a corresponding weight loss of around 5%, accompanied by a small endothermal effect with the maximum at 80 °C. Between 105-200 °C the chemically bonded organics are eliminated from the gel with a corresponding mass loss of around 6% with presence of an exothermic effect at around 190 °C. Also, between 200-500 °C, the structural hydroxyls are eliminated and the residual organics are burned out with a mass loss of around 11% and an exothermal effect at 346 °C.

Fig. 6b shows the X-ray diffraction pattern of the TiO_2 powder, thermally treated at 400 °C, exhibiting diffraction lines at 2θ of 25.26°, 36.89°, 47.96°, 53.91°, 54.93°, 62.65°, 68.58°, 70.19°, 75.10° which are assigned to the crystallographic planes (101), (004), (200), (105), (211), (204), (116), (220), (215) and (224) of the tetragonal crystalline structure of TiO_2-anatase according to JCPDS Card No. 21-1272. The morphology of the TiO_2-anatase (inset of Fig 6b) consists of particle aggregates with quasi-spherical forms with a diameter ranging from about 0.3 to 1.3 microns. Similarly with ZnO, the TiO_2 aggregates exhibit a fine granulation consisting of nanoparticles with size of approximately 10 nm.

The FT-IR spectra of the TiO_2 gel thermally treated at 400 °C for 1 h, are presented in Fig. 6c. The vibration bands around 3400 cm^{-1} and 1627 cm^{-1} are present in the spectra and correspond to hydroxyl groups linked with titanium atoms (Ti-OH) and to surface-adsorbed water.[21] The vibration band at 2369 cm^{-1} can be attributed to physical CO_2 gas absorbed at the surface of material.[22] The vibration band assigned to the Ti-O-Ti network are presented at 484 cm^{-1}, the intensity of this band showing a network ordering.

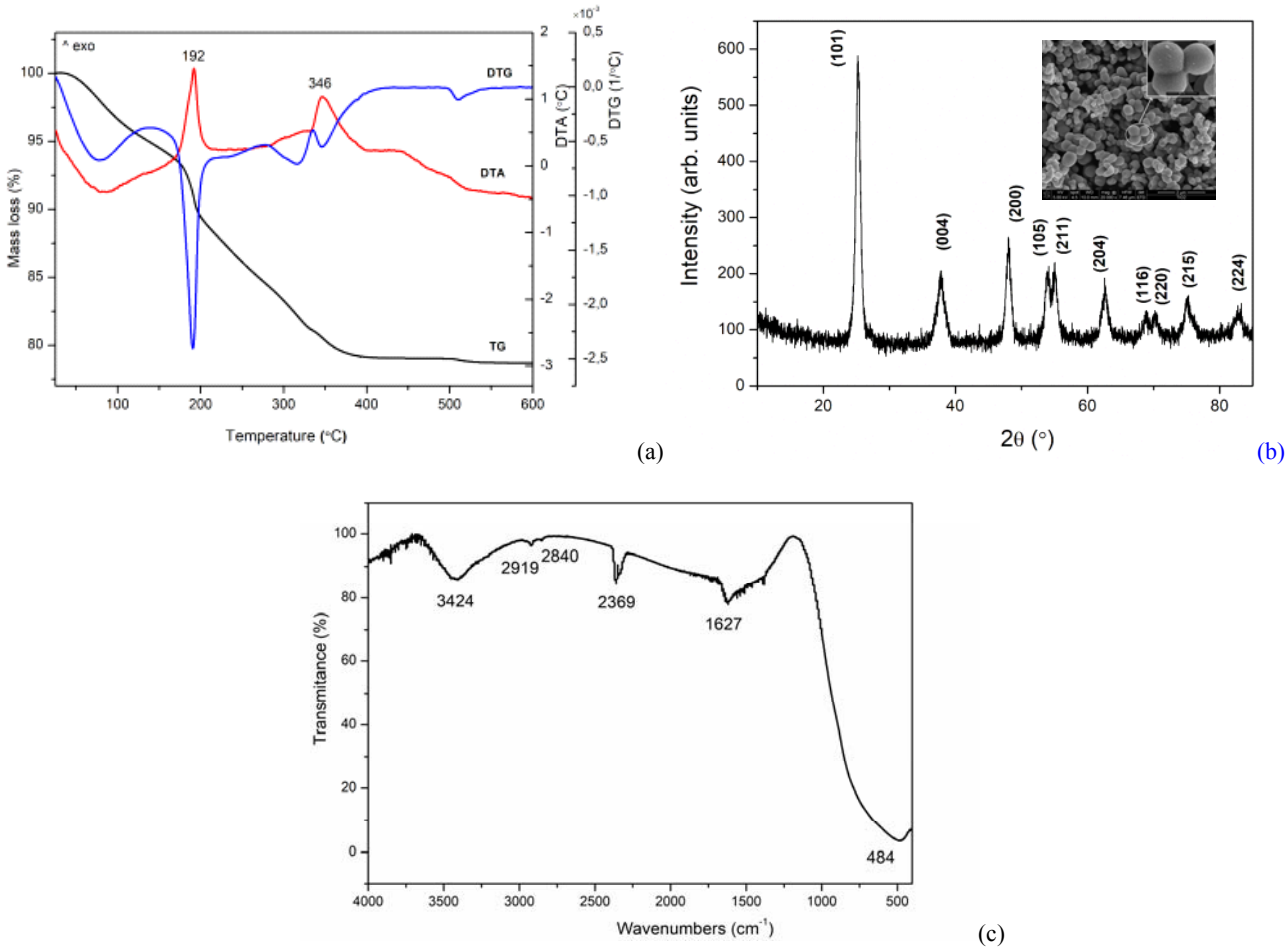

Fig. 6 – (a) ATD, DTG and TG curves for the TiO_2 gel (b) X-ray diffraction patterns of TiO_2 powder in the angular range of 2θ between 5 ° and 85 °; Inset: SEM images of the TiO_2 powder with anatase phase; the inset shows in detail the spherical shape of the constituent particles which have the tendency of merging (c) FT-IR spectra of the gel thermally treated at 400°C for 1 hour.

2. Photocatalytic activity of pristine and Au modified ZnO samples in the Rhodamine B degradation reaction

The photocatalytic activity of undoped ZnO samples was tested in the Rhodamine B degradation reaction. For comparison purposes, the same dye degradation reaction was made in the presence of undoped TiO_2 powder prepared by sol-gel method and thermally treated at 400 ^oC. The photocatalytic activity of the materials was performed using 120 mL of Rhodamine B solution with an initial concentration of 10 mg/L and 0.1 g of a slurry ZnO (or TiO_2) catalyst, by monitoring the evolution of the of Rhodamine B concentration over time. Liquid samples were taken every 30 minutes from the reactor and their absorbance was measured using a UV-VIS-Analtik Jena Specord 200 Spectrophotometer.

After 3 hours of illumination, similar values of Rhodamine B conversion (Table 2) were recorded for undoped TiO_2 (Fig. 7a) and ZnO (Fig. 7b) samples (both of them calcined at 400 ^oC), the conversion being 55% for undoped TiO_2 (calcined at 400 ^oC) and 54% for undoped ZnO calcined at 400 ^oC after 3h of reaction. The photocatalytic degradation of the colorant over time (C_0-C/C_0) x100 was evaluated from the absorbance values which were transformed into conversion values.

TiO_2 is a widely used photocatalyst, and therefore the optimization of synthesis, doping and testing in practical applicability reactions remains an important research topic. From this point of view, the present results consist of encouraging premises, especially for samples containing ZnO, in the subsequent use of these materials in photocatalytic degradation reactions of organic compounds assimilated to various contaminants and in photocatalytic processes involving self-cleaning systems.

Table 2

Evolution of the conversion values for undoped TiO_2 and ZnO powders, both thermally trated at 400 ^oC

Time (min)	TiO_2 $(C_0\text{-}C/C_0)$ x 100	ZnO $(C_0\text{-}C/Co)$x100
0	0	0
30	15.09	7.54
60	16.60	18.11
90	26.03	28.67
120	33.58	38.86
150	44.90	49.05
180	55.09	54.71

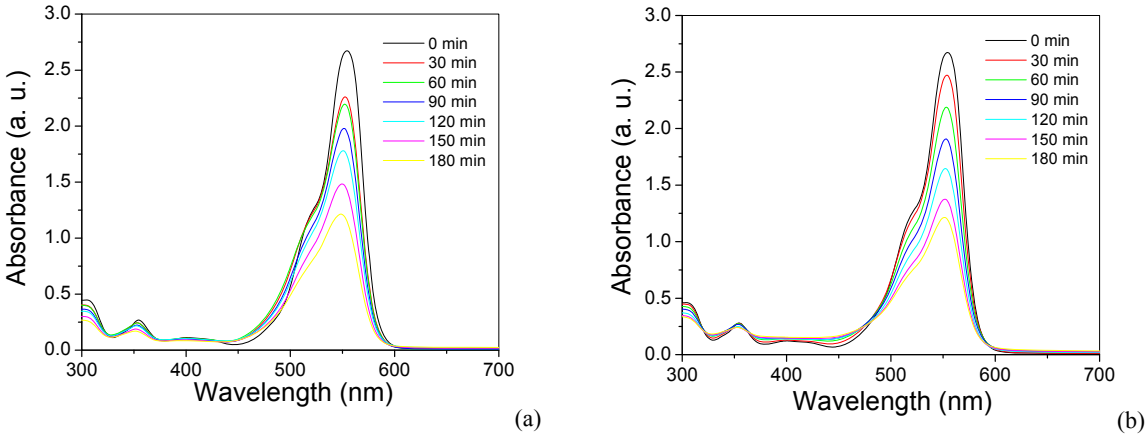

Fig. 7 – The photocatalytic activity of undoped TiO_2-(a) and ZnO-(b), both calcined at 400 ^oC, tested in the RhB degradation reaction, followed by the absorbance decrease over time.

From the data presented in Table 2, a rate constant, k, of app. 0.0051 min^{-1} was calculated for TiO_2 and of app. 0.0049 min^{-1} for ZnO, both materials calcined at 400 ^oC, by considering a pseudo first order kinetic for the RhB photodegradation. In comparison, Rahman et al.[23] reported a rate constant of 0.0343 min^{-1} for the photocatalytic degradation of rhodamine B dye by ZnO nanoparticles with average size of 20–30 nm. The morphology of Rahman's ZnO is very similar with the one we obtained for TiO_2, *i.e.* well dispersed ZnO nanoparticles that does not tend to form large quasi-spherical aggregates, as we obtained for our material (Fig. 4). However, their material has a band gap value of 3.29 eV, corresponding to the wurtzite hexagonal phase of ZnO, which is basically the same we estimated from UV-VIS spectroscopy (Fig. 5). The literature present a wide range of data for the apparent rate constant of the dye degradation, depending on the experimental conditions. For example, the degradation of Methyl Orange (MO) on the TiO_2 Degussa the rate constant (k) was found to be 0.005 min^{-1} while for ZnO treated at 600 ^oC, in the same conditions, a higher value was found: 0.0215 min^{-1}.[20] The values calculated from our tests are pretty similar for TiO_2 and ZnO treated at the same temperature, 400 ^oC.

Further on, it was studied the photocatalytic activity of the ZnO powders thermally treated at 500 ^oC as well as of the Au-modified ZnO powders, also TT at 500 ^oC. In this case, it was used a higher temperature of TT comparing with the previous case, not only to ensure the decomposition of the Au precursor (chloroauric acid) but to determine a better crystallization of the ZnO powders. In this way, it can be observed the influence of the dopant (Au) as well as the crystallinity improvement on the photocatalytic properties of the obtained materials. Indeed, both XRD and FT-IR pointed out a better crystallization than for the undoped ZnO powder which is further improved by Au modification.

The photocatalytic activity of the pristine and Au-modified ZnO powders, TT at 500^{o}C, was tested for Rhodamine B degradation under simulated solar light, in similar conditions to the previously tested ones. The evolution of the conversion values for pristine and Au-modified ZnO powders, both calcined at 500 ^oC, are presented in Table 3. These data have been used to evaluate the kinetics of RhB degradation reaction

over the same materials leading to the following rate constants: 0.0017 min^{-1} for ZnO calcined at 500 ^oC and, respectively 0.0026 min^{-1} for Au-modified ZnO, calcined at the same temperature. It can be said that the modification of the ZnO powder with 0.14 wt % Au exhibit a synergic effect on the ZnO powders thermally treated at 500 ^{o} C, by increasing its capacity for Rhodaminei B photodegradation.

Fig. 8 shows a comparative picture of all investigated materials regarding the conversion of the Rodamine B after 3h of reaction under simulated solar light irradiation. As could be seen from Fig. 8, the dye conversion over undoped TiO_2 and ZnO powders, prepared by sol-gel method and thermally treated at 400 ^oC, reach the same value after 3h of reaction (~55%). In the mean time, surprisingly, the improvement of the crystallinity of the ZnO, after thermal treatment at 500 ^oC, basically leads to a decrease of its photocatalytic activity as the dye conversion decreases to ~27%. Most probably, the thermal treatment at 500 ^oC is resulting both in a decreasing of the surface defects and the reducing of the active photocatalytic reaction sites, that hinder the adsorption of RhB and thus the conversion of the dye but also could be related to the disappearance of the surface bound H_2O/hydroxyl groups from the sample treated at 500^oC (as the FTIR spectra clearly indicated it – Fig. 2) and, consequently, affecting the photogeneration of the hydroxyl radicals HO•, which are usually involved in photodegradation of dyes [21,24]. The relation between the crystallinity, structure of defects and optical (adsorption) properties of the material was also reported by Rahman *et al*.[23].

The lowest conversion of Rhodamine B in the presence of ZnO sample treated at 500 ^oC could be also correlated with XRD data which show the higher crystallite size (222 Å – Table 1). According to literature data, the increasing of the crystallite size promotes the bulk recombination of photogenerated electrons and holes, a decay of photocatalytic activity being presumable.[19]

Table 3

Evolution of the conversion values for pristine and Au-modified ZnO powders, thermally treated at 500 ^oC

Time (min)	ZnO $(C_0\text{-}C/C_0)$ x 100	Au-ZnO $(C_0\text{-}C/Co)$x100
0	0	0
30	7.92	11.25
60	13.05	17.65
90	16.62	24.57
120	20.39	27.44
150	23.66	33.99
180	27.04	38.51

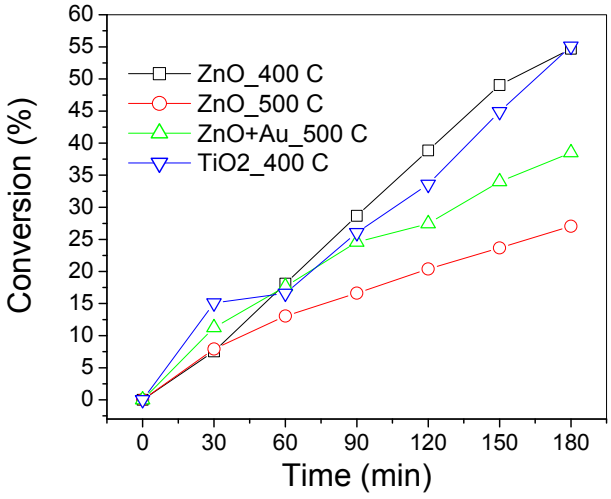

Fig. 8 – Comparative dye conversion under simulated solar light irradiation in the presence of the investigated powders.

On the other hand, the modification with Au improves the performance of the ZnO powder TT at 500 ^{o}C, resulting in the dye conversion up to ~38% after 3h of reaction. According to Fig.5, the presence of Au nanoparticles on the ZnO surface induces the appearance of a plasmonic resonance peak located at 543 nm, showing an improved interaction with light of ZnO based material. (light harvesting behavior). In addition to this, it is well known that the presence of Au nanoparticles deposited on the semiconductor substrate, in this case ZnO, can hinder the recombination of photogenerated carriers, enhancing in this way the photocatalytic activity of the material.[25]

Nevertheless, a significant result of the performed study is that the ZnO powder prepared by sol-gel method and thermally treated at 400 ^{o}C exhibit a similar behavior to that of TiO_2 for the Rh B photodegradation under simulated solar light, thus recommending it as a suitable material for environmental applications. Additionally, it was revealed that the modification of ZnO with Au improves its photocatalytic activity.

CONCLUSIONS

Pristine and Au-modified ZnO powders have been prepared using the sol-gel alcoholic route, which were thermally treated at 400 and 500 ^{o}C. XRD analysis identified the wurtzite phase of ZnO with crystallites size of about 22 nm in all samples. The structural features of ZnO were revealed by FT-IR spectroscopy. The characteristic band at 436 cm^{-1} was assigned to Zn-O bond in wurtzite structure. The intensity of bands in the spectrum of Au-doped ZnO that show the crystallization was influenced by both temperature and Au addition in composition. SEM measurements revealed the morphology of the ZnO powder consisting of globular shaped aggregates, which exhibit nanostructured surfaces covered with small crystallites (tens of nm), in agreement with XRD data. Both XRD and FTIR emphasized the improvement of the ZnO crystallinity after TT at 500 ^{o} C, and after Au-modification. TiO_2 material, used as reference in the present study, has been prepared by sol-gel method and thermally treated at 400 ^{o}C, as suggested by the TG/DTA analysis. XRD and FTIR reveal the characteristic patterns of anatase phase as well as the vibrational bands. SEM micrographs emphasized the fine grain structure of the prepared material, showing the formation of large spherical aggregates, better compacted than in the case of ZnO-based powders.

The photocatalytic activity of ZnO powder was tested for Rhodamine B degradation under solar irradiation for 3h and compared with TiO_2. It was found that the Rhodamine B conversion in the presence of ZnO powder thermally treated at 400 °C was 54% after 3h reaction, similar with TiO_2. The improvement of the ZnO crystallinity by treating the ZnO sample at 500 ^{o}C does not improve its photocatalytic performance, the Au-modification of the ZnO sample brings a higher photocatalytic activity related to the unmodified one, but still remains slightly reduced than that of the samples treated at 400 ^{o}C (ZnO and TiO_2).

Considering these results, ZnO-based materials are recommended both in photocatalytic degradation of various organic compounds and in photocatalytic processes involving self-cleaning systems.

Acknowledgements: Financial support from Project – PN-IIPT-PCCA-2013-4(0864)-(94/2014) – "Cleanphotocoat" is gratefully acknowledged.

REFERENCES

1. L. Schmidt-Mende and J. L. MacManus-Driscoll, *Mat. Today*, **2007**, *10*, 40-48.
2. J. Pan, H. Shen and S. Mathur, *J. Nanotechnology*, **2012**, *2012*, 1-12.
3. E. Bacaksiz, M. Parlak, M. Tomakin, A. Özcelik, M. Karakiz and M. Altunbas, *J. Alloy. Comp.,* **2008**, *466*, 447-450.
4. J. Wang, J. Cao, B. Fang, P. Lu, S. Deng and H. Wang, *Mater. Lett.*, **2005**, *59*, 1405-1408.
5. Z. L. Wang, *ACS Nano*, **2008**, *2*, 1987–1992.
6. Y. Feng, G. Wang, J. Liao, W. Li, C. Chen, M. Li and Z. Li, *Sci. Rep.* **2017,** *7:11622,* 1-10.
7. W. Raza, S. M. Faisal, M. Owais,D. Bahnemann and M. Muneer, *RSC Adv.,* **2016**, *6*, 78335- 78350.
8. C. Anastasescu, N. Spataru, D. Culita, I. Atkinson, T. Spataru, V. Bratan, C. Munteanu, M. Anastasescu, C. Negrila, I. Balint, *Chem. Eng. J.*, **2015**, *281*, 303-311
9. L. Sun, D. Zhao, Z. Song, C. Shan, Z. Zhang, B. Li and D. Shen, *J. Colloid Interface Sci.,* **2011**, *363,* 175–181.
10. H.B. Zeng, P.S. Liu, W.P. Cai, S.K. Yang and X.X. Xu, *J. Phys. Chem*., C **2008**, *112,* 19620–19624.
11. T. Mokari, C.G. Sztrum, A. Salant, E. Rabani and U. Banin, *Nat. Mater*., **2005**, *4* , 855–863.
12. A. Kołodziejczak-Radzimska and T. Jesionowski, *Materials*, **2014**, *7*, 2833-2881.
13. C. Brinker and G. Scherer, "Sol Gel Science: The Physics and Chemistry of Sol Gel Processing", Ed. Academic Press, 1990.
14. C. Anastasescu, S. Mihaiu, S. Preda and M. Zaharescu, "1D Oxide Nanostructures Obtained by Sol-Gel and Hydrothermal Methods", Ed. Springer International Publishing, 2016.
15. I. Stanciu, L. Predoana, S. Preda, M. Anastasescu, J. M. Calderon-Moreno, M. Stoica, M. Gartner, M Zaharescu, *Mat. Sci. Semic. Process.*, **2017**, *68*, 118-127.

16. M. Crişan, M. Raileanu, A. Ianculescu, D. Crisan, N. Dragan, "The Sol-Gel Process: Uniformity, Polymers and Applications", Rachel E. Morris (Ed.), Nova Science Publisher, 2011, p. 1-135.
17. S. Mihaiu, J. Madarasz, G. Pokol, I. M. Szilagyi, T. Kaszas, O. C. Mocioiu, I. Atkinson, A. Toader, C. Munteanu, V. E. Marinescu, M. Zaharescu, *Rev. Roum. Chim.,* **2013,** *58,* 335-345.
18. S. Mihaiu, I.M. Szilagyi, I. Atkinson, O.C. Mocioiu, D. Hunyadi, J. Pandele-Cusu, A. Toader, C. Munteanu, S. Boyadjiev, J. Madarasz, G. Pokol, M. Zaharescu, *J. Therm. Anal. Calorim.*, **2016,** *124*, 71-80.
19. R. Nagaraja, N. Kottam, C.R. Girija, B.M. Nagabhushana, *Powder Technol.*, **2012**, *215-216*, 91-97.
20. C. Tian, Q. Zhang, A. Wu, M. Jiang, Z. Liang, B. Jiang, H. Fu, *Chem. Commun.*, **2012**, *48*, 2858-2860.
21. I. Stanciu, L. Predoana, C. Anastasescu, D.C. Culita, S. Preda, J. Pandele Cusu, C. Munteanu, A. Rusu, I. Balint, M. Zaharescu, *Rev. Roum. Chim.*, **2014**, *59*, 919-929.
22. L. Todan, T. Dascalescu, S. Preda, C. Andronescu, C. Munteanu, D.C. Culita, A. Rusu, R. State, M. Zaharescu, *Ceram. Int.*, **2014**, *40*, 15693-15701.
23. Q. I. Rahman, M. Ahmad, S. K. Misra, M. Lohani, *Mater. Lett.,* **2013**, *91* 170–174.
24. K. Byrappa, A.K. Subramani, S Anada, K.M.Lokanatha Rai, R Dinesh, M Yoshimura, *Bull.Mater. Sci.*, **2006**, *29*, 433-438.
25. V. Subramanian, E.E. Wolf, P.V. Kamat, *J. Phys. Chem. B*, **2001**, *105*, 11439-11446.